

Single-molecule investigation of the impacts of fluorescent DNA-binding proteins on DNA mechanical properties

Yaxi Cheng(成雅茜), Shang Gao(高上), Xianqi Ye(叶贤其), Chuang Tan(谭创), and Jie Ma(马杰)

Citation: Chin. Phys. B, 2025, 34 (**8**): 088702. DOI: 10.1088/1674-1056/addcbd
http://cpb.iphy.ac.cn; http://iopscience.iop.org/cpb

What follows is a list of articles you may be interested in

Combination of density-clustering and supervised classification for event identification in single-molecule force spectroscopy data

Yongyi Yuan(袁泳怡), Jialun Liang(梁嘉伦), Chuang Tan(谭创), Xueying Yang(杨雪滢), Dongni Yang(杨东尼), and Jie Ma(马杰)
Chin. Phys. B, 2023, 32 (**10**): 108702. DOI: 10.1088/1674-1056/acf03e

Single-molecular methodologies for the physical biology of protein machines

Shuang Wang(王爽), Ying Lu(陆颖), and Ming Li(李明)
Chin. Phys. B, 2022, 31 (**12**): 128702. DOI: 10.1088/1674-1056/ac98a2

New insight into the mechanism of DNA polymerase I revealed by single-molecule FRET studies of Klenow fragment

Rokshana Parvin, Qi Jia(贾棋), Jianbing Ma(马建兵), Chunhua Xu(徐春华), Ying Lu(陆颖), Fangfu Ye(叶方富), and Ming Li(李明)
Chin. Phys. B, 2022, 31 (**8**): 088701. DOI: 10.1088/1674-1056/ac6ed5

Interaction between human telomeric G-quadruplexes characterized by single molecule magnetic tweezers

Yi-Zhou Wang(王一舟), Xi-Miao Hou(侯锡苗), Hai-Peng Ju(车海鹏), Xue Xiao(肖雪), Xu-Guang Xi(奚绪光), Shuo-Xing Dou(窦硕星), Peng-Ye Wang(王鹏业), Wei Li(李伟)
Chin. Phys. B, 2018, 27 (**6**): 068701. DOI: 10.1088/1674-1056/27/6/068701

Bio-macromolecular dynamic structures and functions, illustrated with DNA, antibody, and lipoprotein

Lu Gou(缑璐), Taoli Jin(金桃丽), Shuyu Chen(陈淑玉), Na Li(李娜), Dongxiao Hao(郝东晓), Shengli Zhang(张胜利), Lei Zhang(张磊)
Chin. Phys. B, 2018, 27 (**2**): 028708. DOI: 10.1088/1674-1056/27/2/028708

RAPID COMMUNICATION

Single-molecule investigation of the impacts of fluorescent DNA-binding proteins on DNA mechanical properties

Yaxi Cheng(成雅茜)[1,2], Shang Gao(高上)[1,2], Xianqi Ye(叶贤其)[1,2], Chuang Tan(谭创)[1,2,†], and Jie Ma(马杰)[1,2,‡]

[1] *School of Physics, Sun Yat-sen University, Guangzhou* 510275, *China*

[2] *State Key Laboratory of Optoelectronic Materials and Technologies, Sun Yat-sen University, Guangzhou* 510006, *China*

(Received 15 March 2025; revised manuscript received 7 May 2025; accepted manuscript online 23 May 2025)

DNA imaging and visualization techniques are crucial in biological experiments and have also emerged as a powerful method for single-molecule studies. Traditional intercalating dyes (e.g., SYTOX, EtBr, GelRed) can stain DNA but may alter its structure and mechanical properties, and cause photocleavage. Recently, a novel fluorescent DNA-binding protein (FP-DBP) was introduced, which can stain DNA without sequence preference and without inducing photocleavage. In this study, using a custom-built magnetic tweezers system, we performed DNA stretching, twisting and unzipping experiments to compare the mechanical properties of DNA with and without two kinds of intercalating dyes (SYTOX Orange and GelRed) and mCherry FP-DBP. Our results show that mCherry FP-DBP does not affect DNA structure or mechanics, unlike SYTOX Orange and GelRed, making FP-DBP a promising tool for DNA visualization in single-molecule experiments.

Keywords: fluorescent DNA-binding protein, single-molecule, magnetic tweezers, DNA mechanical properties, intercalating dye

PACS: 87.80.Nj, 82.37.Rs, 87.14.gk, 87.15.La

DOI: 10.1088/1674-1056/addcbd **CSTR:** 32038.14.CPB.addcbd

1. Introduction

The techniques of DNA imaging and visualization have been extensively employed in a variety of biological experiments, including gel electrophoresis and fluorescence *in situ* hybridization (FISH) assays.[1–4] Recently, these techniques have also emerged as crucial tools in single-molecule studies. For instance, in DNA curtain experiments, stained DNA molecules can be utilized to monitor the activities of a single enzyme.[5] In DNA stretching experiments, the integration of optical tweezers (OT)[6] or flow cell[7] with fluorescence microscopy enables direct visualization of DNA structural changes under different tensions. Besides, DNA visualization techniques have also been used to observe the dynamics of DNA supercoils.[8,9] All these experiments have allowed researchers to examine biological processes in unprecedented detail.

In most of the previously mentioned experiments, the visualization of DNA involves the use of intercalating dyes, such as SYTOX, YOYO, EtBr and GelRed, to stain the DNA. These dye molecules typically possess one aromatic group (mono-intercalators) or two (bis-intercalators), which insert between DNA bases.[10] Consequently, the binding of these dyes often modifies the DNA structures and mechanical responses. For instance, the binding of SYTOX or YOYO dyes can significantly distort the DNA stretching curve.[11] Additionally, intercalated dyes like EtBr have been demonstrated to unwind DNA and substantially impact the DNA winding curve.[12] Given that DNA structure and mechanical properties are crucial in DNA–protein interactions, this poses a significant limitation for using these dyes to visualize DNA and DNA–protein interactions. Furthermore, these intercalation dyes are also known to cause DNA photocleavage,[13] further restricting their applications in DNA imaging and visualization.

Interestingly, a recent report by Lee *et al.*[13] introduced a novel design of a fluorescent DNA-binding protein (FP-DBP) that holds promise in addressing these challenges. The FP-DBP comprises a fluorescent protein flanked by two small peptides (KWKWKKA) on each side, which utilize lysine to bind to DNA phosphates and tryptophan to intercalate between DNA bases. Consequently, it has been demonstrated to effectively 'paint' entire DNA molecules without sequence preference. Besides, even without an anti-bleaching agent, FP-DBPs have been shown to induce no photocleavage, as the DNA binding moiety of the FP is effectively isolated from the fluorophore moiety. Furthermore, a comparison of the contour length of λ-DNA stained with FP-DBP versus YOYO-1 revealed that the former well aligns with the expected DNA contour length, whereas the latter significantly exceeds it. Based on these observations, it was postulated that FP-DBP does not disrupt DNA structures despite intercalation. However, to

†Corresponding author. E-mail: tanch26@mail.sysu.edu.cn

‡Corresponding author. E-mail: majie6@mail.sysu.edu.cn

© 2025 Chinese Physical Society and IOP Publishing Ltd. All rights, including for text and data mining, AI training, and similar technologies, are reserved.

draw a conclusion on this still needs more accurate measurements. Besides, whether FP-DBP influences DNA mechanical responses remains largely unknown. Clarification of these questions also requires more quantitative evidences from experiments.

In this study, we aimed to elucidate whether FP-DBP alters DNA structure and impacts its mechanical properties. Initially, we utilized a flow-cell to demonstrate the binding capability of purified mCherry fluorescent DNA-binding protein (mCherry FP-DBP) to DNA. Subsequently, we employed a custom-built magnetic tweezers (MT) system to quantitatively characterize the stretching, twisting and unzipping mechanics of DNA in the absence and presence of intercalating dyes (such as SYTOX Orange and GelRed) and mCherry FP-DBP. Our findings reveal that mCherry FP-DBP has no effect on DNA structures and mechanical responses, in stark contrast to SYTOX Orange and GelRed. These results establish FP-DBP as a promising tool for DNA visualization in single-molecule experiments.

2. Methods

2.1. Sample preparation

2.1.1. Purification of mCherry fluorescent DNA-binding protein

The mCherry FP-DBP, containing one peptide (KWKWKKA) at each terminal, was expressed and purified as previously described.[13] Briefly, the plasmid pET-2(KW)2-mCherry (Addgene) was transformed into *E. coli* BL21(DE3) for protein overexpression. Cells were grown in LB media supplemented with 100 μg/ml of ampicillin at 37 °C until the $OD_{600\ nm}$ reached ∼ 0.8, and then were induced with 1 mM of IPTG (Sangon Biotech, A600168-0005). After induction at 18 °C for additional 24 hours, the cells were harvested by centrifugation (12000 × *g*) for 20 min and stored at −80 °C. The frozen cell pellet was thawed on ice and re-suspended in lysis buffer (50 mM Na_2HPO_4, 300 mM NaCl, 10 mM Imidazole, pH 8.0) with EDTA-free protease-inhibitor cocktail (MCE, HY-K0011). The suspended cells were lysed by sonication for one hour, and the cell debris was pelleted by centrifugation (15000 × *g*) for 30 min at 4 °C. The supernatant was cleared by passing through a 0.45-μm filter (Millipore, SLHV004SL), and loaded onto a HisTrap HP column (Cytiva, 17524701) at the rate of 0.3 mL/min. The column was further rinsed twice with wash buffer (50 mM Na_2HPO_4, 300 mM NaCl, 20 mM Imidazole, pH 8.0), and the bound proteins were eluted in elution buffer (50 mM Na_2HPO_4, 300 mM NaCl, 250 mM Imidazole, pH 8.0). Finally, the purified proteins were dialyzed into storage buffer (50 mM Na_2HPO_4, 300 mM NaCl, 50% v/v glycerol, pH 8.0) and stored at −20 °C.

2.1.2. Preparation of DNA templates for single-molecule experiments

Three distinct DNA templates were specifically designed for different single-molecule experiments. The λ-DNA with multiple biotin-tags at both termini was utilized for single-molecule fluorescence imaging; the 13-kb DNA containing multiple biotin- and digoxigenin-tags at opposing ends was engineered for single-molecule fluorescence imaging, stretching and twisting experiments; and the T-DNA was synthesized for unzipping experiments. Detailed protocols for the preparation and functionalization of these DNA constructs are provided in the SI Appendix.

2.2. Flow-cell setup

The home-built flow-cell setup, which has been previously reported,[7] comprises a flow-cell system, a fluorescence microscope, and a CMOS camera. The flow-cell system consists of several components: a gas pump controller (PC1, FluidicLab, Shanghai, China), a flow meter (FS4A, FluidicLab, Shanghai, China), and a flow-cell chamber constructed from a 24 mm × 60 mm coverslip and a 25.4 mm × 76.2 mm microscope slide. During experiments, an increase in gas pressure causes buffer to flow into the chamber, and the flow rate is measured by the flow meter. The fluorescence microscope is equipped with a commercial inverted microscope (Ti2U, Nikon Instruments, Tokyo, Japan), a high-resolution 60×, 1.45-NA oil immersion objective lens (Nikon Instruments, Tokyo, Japan), and an excitation laser sourced from Changchun New Industries Optoelectronics Technology in Changchun, China. High-sensitivity fluorescence images are captured by a CMOS camera (Prime 95B, Teledyne Photometrics, Tucson, AZ).

2.3. Magnetic tweezers

The customized magnetic tweezers system[14] comprises a Nikon inverted microscope (Ti2U, Nikon Instruments, Tokyo, Japan) equipped with a high-resolution 60×, 1.45-NA oil immersion objective lens (Nikon Instruments, Tokyo, Japan). Permanent magnets are mounted on the top of the microscope to apply forces to the sample. An LED light source positioned above the magnets provides illumination, while a CMOS camera (EoSens 3CL, Mikrotron, Gilching, Germany) is connected to the microscope for imaging and bead tracking. Prior to each measurement, a calibration procedure is conducted. This involves setting up a calibration table that documents the image contrasts of a reference bead stuck to the coverslip and selected beads at different heights relative to the focal plane of the objective.

2.4. DNA imaging experiment

In the DNA imaging experiment, λ-DNA with multiple biotin tags was immobilized onto the coverslip through inter-

actions between biotin and neutravidin which was connected to biotin-LC-BSA coated on the coverslip surface, while 13-kb DNA molecules were tethered between the coverslip via digoxigenin and anti-digoxigenin interactions. Following this, fluorescence images were captured under total internal reflection fluorescence (TIRF) illumination mode with a 532 nm laser for excitation. The laser output power was set to approximately 10 mW, and the camera exposure time was set to 10 ms. To obtain clear images of the stretched DNA, the flow rate was adjusted to 70 μL/min for λ-DNA and 125 μL/min for 13-kb DNA. For the flowing buffer, a concentration of 10 nM mCherry FP-DBP diluted in TE buffer (10 mM Tris-HCl, 1 mM EDTA, pH 8.0) was used for both λ-DNA and 13-kb DNA.

2.5. DNA stretching experiment

In the DNA stretching experiment, prior to forming the 13-kb DNA tethers, we initially functionalized the coverslip surface with 0.02 mg/ml anti-digoxigenin. Subsequently, we stuck the reference beads (2.9 μm polystyrene beads) to the coverslip surface. Following this, the coverslip surface was passivated using a 6 mg/ml casein solution. Afterwards, 5 pM DNA was introduced and immobilized on the coverslip surface through its digoxigenin tag at one end. Finally, the DNA tethers were formed by introducing streptavidin-coated superparamagnetic beads (Dynabeads M270) to connect with the biotin tag at the other end of the DNA. During the DNA stretching experiment, we utilized MT to first stretch the anchored 13-kb DNA molecules in TE buffer. Subsequently, the buffer was replaced with TE solutions containing varying concentrations of SYTOX Orange (Invitrogen, S11368), GelRed (Biotium, 41003), and FP-DBP, respectively. Once the buffer was changed, we allowed a minimum of 10 min to ensure that the binding had reached an equilibrium before commencing a new measurement of the force-extension curves (FECs) of the DNA.

2.6. DNA twisting experiment

The tether formation procedures for the DNA twisting experiment were identical to those used in the DNA stretching experiment. We specifically selected tethers that exhibited torsional constraints, meaning the DNA formed multiple attachments to both the coverslip surface and the magnetic beads, for the subsequent DNA twisting experiments. Once such a tether was identified, we rotated the magnets in the magnetic tweezers at 0.5 Hz to twist the 13-kb DNA while maintaining a constant force (e.g., 0.2 pN). This allowed us to obtain DNA twisting curves, which represent the relationship between DNA extension and the number of magnet rotations. In the experiments, we initially measured the DNA twisting curves in TE buffer. Subsequently, we replaced the buffer with TE solutions containing different concentrations of SYTOX Orange, GelRed, and FP-DBP, respectively, before repeating the measurement of the DNA twisting curves.

2.7. DNA unzipping experiment

The tether formation procedures for the DNA unzipping experiment were analogous to those employed in the DNA stretching experiment, with the exception that T-DNA (DNA hairpin) was utilized as the DNA sample. During the DNA unzipping experiment, the T-DNA was stretched to 30 pN and subsequently relaxed to 0 pN. The stretching–relaxation curves of the DNA were then measured. The unzipping force was determined by the force at which a sudden increase in extension occurred during the unzipping process, while the rezipping force was derived from the force at the onset of an abrupt decrease during the rezipping process. For each concentration of staining dye or FP-DBP, we analyzed at least twelve independent molecules to calculate the average unzipping force, rezipping force, and their respective standard deviations.

3. Results and discussion

3.1. DNA staining with purified FP-DBP

We firstly demonstrated the capability of our purified mCherry FP-DBP to successfully stain DNA of varying lengths. As illustrated in Fig. 1(a), we employed a flow-cell technique to stretch DNA tethered to the coverslip surface. The details about our flow-cell setup and experiment procedures have been described previously and also introduced in SI Appendix. Upon introducing 10 nM FP-DBP into the chamber, both λ-DNA and 13-kb DNA were stained and clearly visualized, as depicted in Figs. 1(b) and 1(c). Notably, we observed that the binding affinity of FP-DBP to DNA is sensitive to the salt concentration, with an increase in Na^+

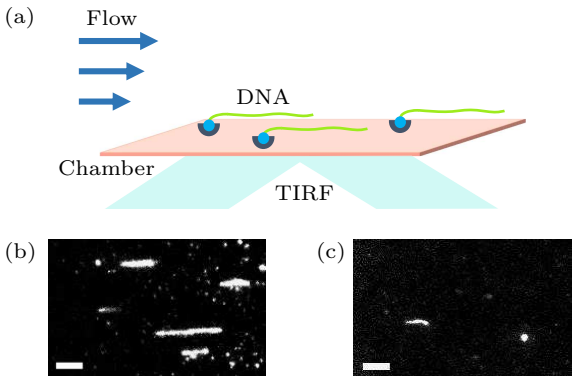


Fig. 1. The schematics of flow-cell experimental configuration. DNA was anchored to the surface of coverslip via the interaction between biotin/digoxigenin (light blue) and neutravidin/anti-digoxigenin (dark blue) and then stretched by flow, followed by fluorescence imaging under TIRF illumination. (b) The fluorescence image of the stretched single λ-DNA molecules under a flowing buffer containing 10 nM mCherry FP-DBP. (c) The fluorescence image of the stretched 13-kb DNA molecule under a flowing buffer containing 10 nM mCherry FP-DBP. The scale bars in (b) and (c) represent a length of 5 μm.

concentration beyond 10 mM almost resulting in the elimination of staining. This observation indicates that the binding of FP-DBP to DNA largely depends on electrostatic interactions between its lysine segment and the phosphate of DNA, while the intercalation of tyrosine between DNA bases may play a less important role. On one hand, this characteristic poses certain limitations on the applications of FP-DBP. On the other hand, it also brings some flexibility such as making FP-DBP staining easily reversible.

3.2. DNA stretching in presence of FP-DBP

To quantify the influence of FP-DBP on DNA stretching mechanics, we performed DNA stretching experiments using custom-made magnetic tweezers, as illustrated in Fig. 2(a). Details regarding this setup have been previously reported[14] and further described in Section 2. For comparison, we first selected SYTOX Orange (a mono-intercalator)[11] and GelRed (a bis-intercalator),[15] both commonly used intercalating dyes for DNA staining, to investigate their effects on DNA mechanical properties. The force–extension curves (FECs) obtained both with and without these dyes are presented in Figs. 2(b) (SYTOX Orange) and 2(c) (GelRed). The concentrations of SYTOX Orange utilized here were 10 nM and 100 nM. For GelRed, we chose concentrations of 1 nM and 10 nM. It should be noted that in many DNA visualization experiments (such as DNA curtain experiments), the concentrations of commonly employed dyes, such as YOYO and SYTOX, typically fall within the range of sub-nanomolar (nM) to several nanomolar.[5–7,16] Some studies[6,7] have demonstrated that SYTOX dyes at 1–2 nM concentrations exert minimal perturbation on DNA stretching curves, thereby ensuring the reliability of experimental results in such cases. However, there are also some DNA imaging experiments[9,11,17] that do use relatively higher concentrations of dyes and those concentrations fall within the range tested here. As demonstrated in Fig. 2(b), at 10 nM condition, the intercalation of SYTOX Orange significantly altered the DNA FEC, causing DNA elongation and enhancing the overstretching transition force. Ultimately, at 100 nM SYTOX Orange, the overstretching transition "plateau" completely disappeared. Similarly, under both 10 nM and 1 nM conditions, GelRed intercalation also markedly elongated DNA and modified the overstretching transition region in the FEC. In stark contrast, the typical stretching and relaxing curves for DNA with 100 nM

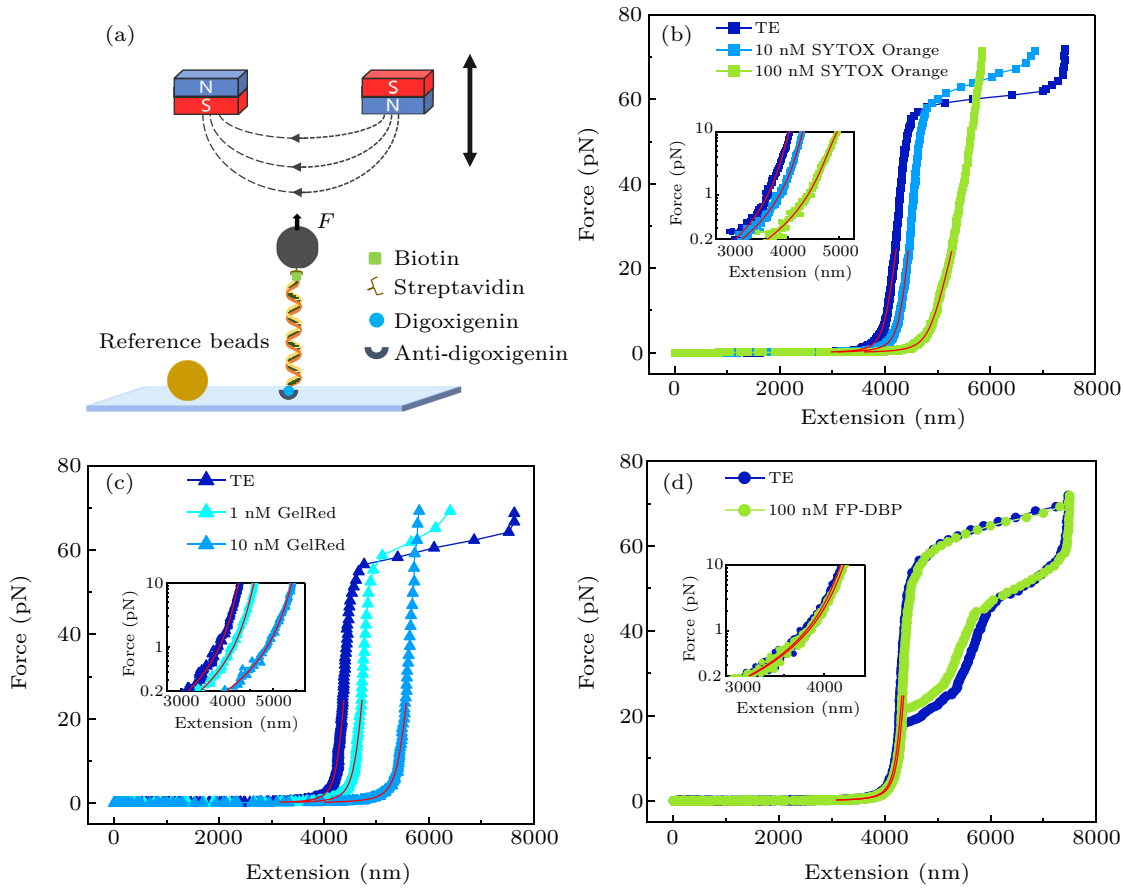


Fig. 2. (a) The schematics of DNA stretching experimental configuration. A 13-kb DNA molecule is immobilized on the surface via the linker at one end and connected with a magnetic bead via the linker at the other end. Later, it can be stretched using MT. (b)–(d) The measured stretching and relaxing curves of the same DNA molecule under different concentrations of SYTOX Orange, GelRed and mCherry FP-DBP, respectively. The red lines represent the fitting curves using Odijk WLC model for the data in the stretching curves within the force range of 0.2–25 pN. The fitting results are summarized in Tables S3-S5. The insets show the stretching curves along with their corresponding fitting curves, with the force plotted on a logarithmic scale (base 10).

Table 1. The measured DNA structural and mechanical parameters from fitting DNA stretching curves with the Odijk WLC model[18,19] (0.2–25 pN). The values are the mean ± the standard error of the mean (SE).

FP-DBP concentration (nM)	L (nm)	d (nm/bp)	L_p (nm)	K (pN)
0	4247.1 ± 35.5	0.327 ± 0.003	49.9 ± 2.4	625.5 ± 49.4
10	4194.7 ± 38.9	0.323 ± 0.003	43.4 ± 4.2	692.8 ± 107.5
100	4211.5 ± 44.0	0.324 ± 0.003	55.1 ± 4.0	690.3 ± 130.3

FP-DBP closely resembled those observed without FP-DBP, as shown in Fig. 2(d). Such a concentration of FP-DBP has been established as sufficient for DNA staining based on the results of Fig. 1. Furthermore, by fitting the measured DNA stretching curves to Odijk WormLikeChain (WLC) model,[18,19] we derived DNA structural and mechanical parameters including contour length (L), base-pair spacing (d), persistent length (L_p), and stretching modulus (K). As shown in Table 1, the average values of these parameters, obtained from 12–18 tethers with and without FP-DBP, are close to each other considering the error bar, with L_p falling within 43–55 nm and K falling within 600–700 pN. We also attempted to fit the same data using a modified WLC model proposed by Bouchiat *et al.*,[20] following the method reported by Shon *et al.*[21] This approach also yielded consistent L_p values of 35–39 nm and K values of 594–784 pN for the buffers with and without FP-DBP. Further details regarding these different fitting methods and results can be found in the supplementary information (SI). Consequently, we conclude that FP-DBP staining introduces no discernible perturbations to DNA stretching mechanics. Intriguingly, we also observed that FP-DBP binding to DNA did not affect the hysteresis between stretching and relaxing curves, which typically reflects the processes of DNA unpeeling during overstretching transition and reannealing during relaxation. Such an observation may suggest that the binding of FP-DBP to single-stranded DNA (ssDNA) is even weaker in comparison with double-stranded DNA (dsDNA) (possibly due to the loss of tyrosine intercalation), thereby not disrupting DNA reannealing.

3.3. DNA twisting in presence of FP-DBP

To assess the influence of FP-DBP on DNA twisting mechanics, we first constructed torsionally-constrained DNA tethers by utilizing digoxigenin and biotin tags on the DNA to form multiple links with anti-dig molecules on the coverslip surface and streptavidin molecules on the magnetic bead,

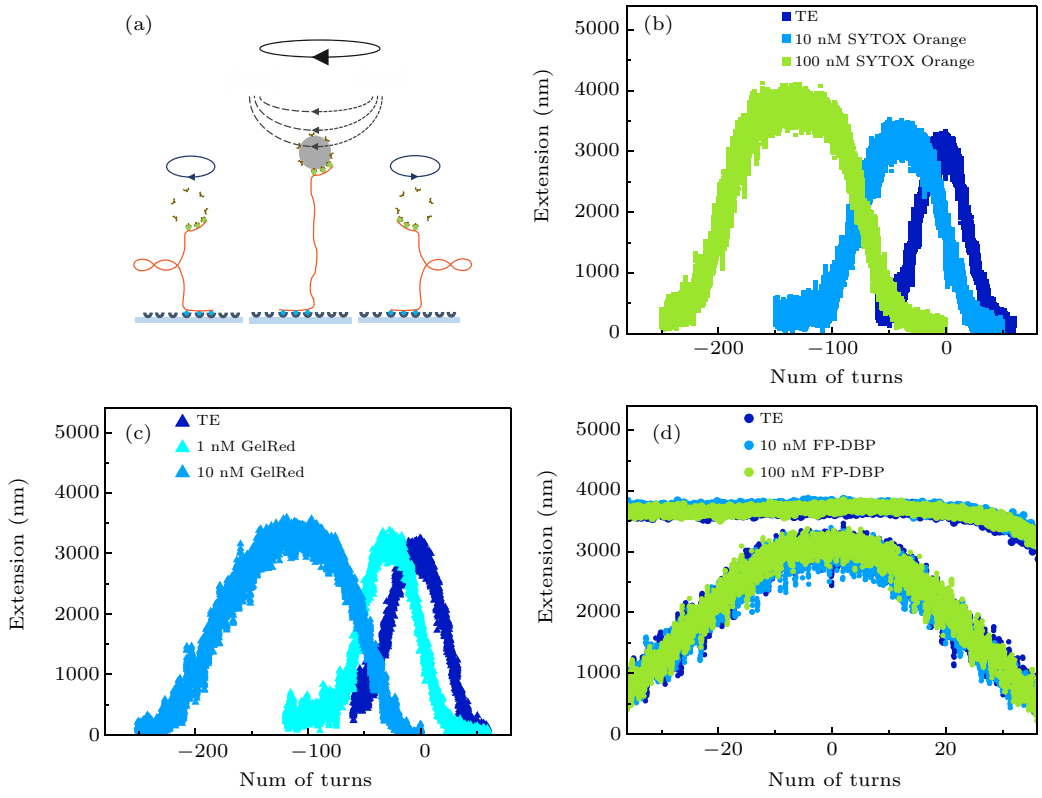


Fig. 3. (a) The schematics of DNA twisting experimental configuration. DNA was torsionally connected with magnetic bead and coverslip surface through the multiple linkers on each end. Later, it can be twisted using MT. (b) The twisting curves of the same 13-kb DNA molecule under a constant force of 0.2 pN with different concentrations of SYTOX Orange, TE: unwinding from 60 turn to −60 turn, 10 nM: unwinding from 50 turn to −150 turn, 100 nM: unwinding from 0 turn to −250 turn. (c) The twisting curves of the same 13-kb DNA molecule under a constant force of 0.2 pN with different concentrations of GelRed, TE: unwinding from 60 turn to −60 turn, 1 nM: unwinding from 60 turn to −120 turn, 10 nM: unwinding from 0 turn to −250 turn. (d) The twisting curves of the same 13-kb DNA molecule under two constant forces (upper: 1.0 pN, lower: 0.2 pN) with different concentrations of mCherry FP-DBP, all curves were unwound from 38 turn to −38 turn.

as depicted in Fig. 3(a). Subsequently, we utilized magnetic tweezers to wind the DNA and measured the DNA twisting curves under constant forces, both in the absence and presence of staining dyes (SYTOX Orange and GelRed) and FP-DBP. Specifically, we started from 0 turn (for 100 nM SYTOX Orange and 10 nM GelRed cases) or first wound DNA for 38–60 turns (for other cases), then unwound DNA for 76–250 turns to get a full twisting curve as shown in Figs. 3(b)–3(d). After that, we rewound DNA back to 0 turn.

As illustrated in Figs. 3(b) and 3(c), upon the addition of both SYTOX Orange and GelRed, a notable shift towards a negative number of winding turns is observed at the maxima of the DNA twisting curve, suggesting that DNA becomes positively supercoiled prior to twisting due to the intercalation of these dyes. In sharp contrast, when FP-DBP is introduced, the twisting curves exhibit minimal deviation. Therefore, our findings demonstrated that FP-DBP staining has negligible influence on DNA twisting mechanics. This characteristic is particularly advantageous when combining FP-DBP with side-pulling MT for visualizing DNA supercoils and studying the dynamics of DNA supercoiling as it allows for independent control of DNA visualization and DNA supercoiling.

3.4. DNA unzipping in presence of FP-DBP

We further utilized MT and DNA hairpin to investigate whether FP-DBP staining could impact DNA unzipping mechanics. The experimental setup is illustrated in Fig. 4(a). The typical FECs measured in the presence or absence of staining dyes and FP-DBP are displayed in Fig. 4(b). From these FECs, we extracted the unzipping and rezipping forces, as indicated in Fig. 4(b). The mean unzipping and rezipping forces at various dye and FP-DBP concentrations are plotted in Figs. 4(c)–4(e). Our results reveal that intercalating dyes such as SYTOX Orange and GelRed could enhance the unzipping force of the DNA hairpin, with the enhancement becoming more pronounced as their concentrations increase. However, the rezipping force appears insensitive to the presence of intercalating dyes, which aligns with the fact that binding to ssDNA is much more difficult than to dsDNA for these dyes. Despite this, our findings demonstrate that commonly used staining dyes like SYTOX Orange and GelRed do modify DNA unzipping mechanics. Conversely, as shown in Fig. 4(e), the binding of FP-DBP to DNA has little effect on either the average unzipping or rezipping forces, suggesting that FP-DBP does not disturb DNA unzipping mechanics.

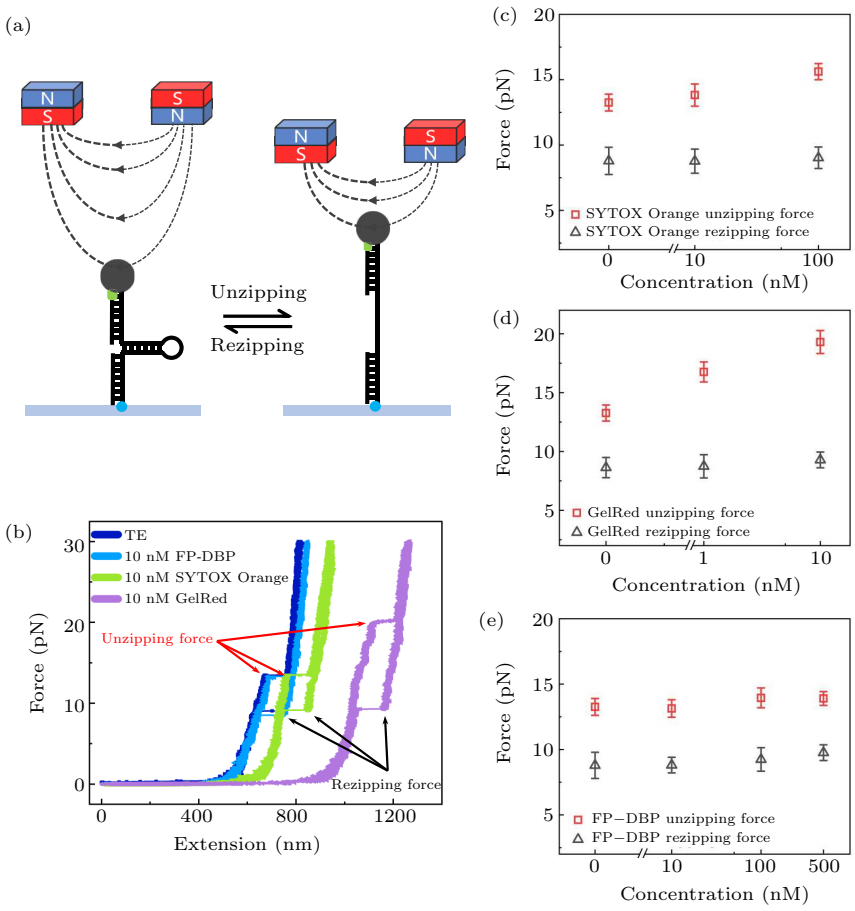


Fig. 4. (a) The schematics of DNA unzipping experimental configuration. DNA molecule containing a 125-bp hairpin structure was immobilized on the surface via the linker at one end and connected with a magnetic bead via the linker at the other end. Later the hairpin structure can be unzipped or rezipped using MT. (b) The typical unzipping and rezipping curves in the absence and presence of the intercalating dyes (SYTOX Orange or GelRed) and mCherry FP-DBP. The red and black arrows indicate the unzipping and rezipping forces, respectively. (c)–(e) The measured mean unzipping and rezipping forces at different concentrations of SYTOX Orange, GelRed and mCherry FP-DBP, respectively.

4. Conclusion

In this study, we have quantitatively measured and analyzed the mechanical responses of DNA to stretching, twisting and unzipping upon the binding of FP-DBP. Our findings reveal that FP-DBP binding to DNA does not modify DNA structures nor disrupt the mechanical properties associated with stretching, twisting and unzipping, standing in marked contrast to commonly utilized intercalating dyes such as SYTOX Orange and GelRed for DNA staining. Considering the pivotal role of DNA mechanical properties in protein-DNA interactions, this unique characteristic positions FP-DBP as a promising candidate for many single-molecule experiments. For instance, we discovered that intercalating dyes like SYTOX Orange and GelRed augment the force required to unzip DNA, indicating that their intercalation reinforces the base-pair energy within DNA. This enhancement may pose challenges in experiments using DNA visualization techniques to investigate helicase activities on DNA unwinding.[5,22] In the context of these experiments, DNA staining with FP-DBP could potentially serve as a useful alternative in the future.

Secondly, our experimental results indicate that mCherry FP-DBP binds to DNA primarily through electrostatic interactions, rendering it sensitive to the salt concentration of the buffers. While this characteristic may pose some limitations on the applications of FP-DBP, it also offers a valuable advantage: the stained FP-DBP can be readily removed and the DNA can be re-stained. This feature is particularly beneficial in single-molecule experiments where certain enzyme activities are very sensitive to staining. For this case, after examining the DNA status (such as DNA supercoiling), FP-DBP can be easily rinsed out, allowing for the subsequent addition of enzymes in further experiments.

Finally, since DNA supercoiling plays an important role in gene regulation,[23–26] it is useful to directly visualize DNA supercoils. Previously, van Loenhout *et al.*[8] utilized side-pulling magnetic tweezers (MT) combined with fluorescence to visualize DNA supercoil dynamics. In their experiments, the purified DNA constructs were covalently labeled with Cy3 using a labeling reagent. Although this labeling was later shown to have no effect on DNA twisting curves, its impact on DNA stretching mechanics remains uncertain. Additionally, the Cy3 labeling is not erasable. Subsequently, another high-throughput single-molecule assay named "Intercalation-induced Supercoiling of DNA" (ISD)[9] was developed for real-time visualization of supercoiled DNA molecules. However, this method necessitates the use of intercalating dyes to induce DNA supercoiling and lacks precise control over DNA supercoiling degree compared to magnetic tweezers. Furthermore, DNA supercoiling induction and visualization are coupled in ISD, limiting independent control. In contrast, FP-DBP staining offers various advantages, including no perturbation to DNA structure and mechanical properties (thereby allowing independent control of DNA supercoiling and visualization when combined with MT), erasability, and compatibility with in vivo assays. Therefore, we anticipate that FP-DBP staining, especially when combined with side-pulling MT, as a promising approach for visualizing DNA supercoils in the future.

Acknowledgments

This project was supported by the National Natural Science Foundation of China (Grant No. 32371284) and the Open Fund of the State Key Laboratory of Optoelectronic Materials and Technologies, Sun Yat-sen University (Grant No. OEMT-2024-ZTS-04). We also wish to thank for the support from the Physical Research Platform in the School of Physics, Sun Yat-sen University (Grant No. PRPSP, SYSU).

References

[1] Seeman N C, Chen J H and Kallenbach N R 1989 *Electrophoresis* **10** 345
[2] Stellwagen N C 2009 *Electrophoresis* **30** S188
[3] Chrzanowska N M, Kowalewski J and Lewandowska M A 2020 *Molecules* **25** 1864
[4] Matsumoto K and Hirose S 2004 *J. Cell Sci.* **117** 3797
[5] Finkelstein I J, Visnapuu M L and Greene E C 2010 *Nature* **468** 983
[6] King G A, Gross P, Bockelmann U, Modesti M, Wuite G J L and Peterman E J G 2013 *Proc. Natl. Acad. Sci. USA* **110** 3859
[7] Zou Z, Liang J, Jia Q, Bai D, Xie W, Wu W, Tan C and Ma J 2023 *Nanoscale* **15** 17443
[8] van Loenhout M T, de Grunt M V and Dekker C 2012 *Science* **338** 94
[9] Ganji M, Kim S H, van der Torre J, Abbondanzieri E and Dekker C 2016 *Nano Lett.* **16** 4699
[10] Almaqwashi A A, Paramanathan T, Rouzina I and Williams M C 2016 *Nucleic Acids Res.* **44** 3971
[11] Biebricher A S, Heller I, Roijmans R F, Hoekstra T P, Peterman E J and Wuite G J 2015 *Nat. Commun.* **6** 7304
[12] Celedon A, Wirtz D and Sun S 2010 *J. Phys. Chem. B* **114** 16929
[13] Lee S, Oh Y, Lee J, Choe S, Lim S, Lee H S, Jo K and Schwartz D C 2015 *Nucleic Acids Res.* **44** e6
[14] Gao S, Liang J, Tan C and Ma J 2025 *Nanoscale* **17** 3236
[15] Crisafuli F A, Ramos E B and Rocha M S 2015 *Eur. Biophys. J.* **44** 1
[16] Kopuštas A, Ivanovaitė Š, Rakickas T, Počevičiutė E, Paksaitė J, Karvelis T, Zaremba M, Manakova E and Tutkus M 2021 *Langmuir* **37** 3428
[17] Janissen R, Barth R, Polinder M, van der Torre J and Dekker C 2024 *Nucleic Acids Res.* **52** 1677
[18] Odijk T 1995 *Macromolecules* **28** 7016
[19] Fu H, Zhang C, Qiang X W, Yang Y J, Dai L, Tan Z J and Zhang X H 2020 *Phys. Rev. Lett.* **124** 058101
[20] Bouchiat C, Wang M D, Allemand J F, Strick T, Block S M and Croquette V 1999 *Biophys. J.* **76** 409
[21] Shon M J, Rah S H and Yoon T Y 2019 *Sci. Adv.* **5** eaav1697
[22] Yardimci H, Wang X, Loveland A B, Tappin I, Rudner D Z, Hurwitz J, van Oijen A M and Walter J C 2012 *Nature* **492** 205
[23] Liu L F and Wang J C 1987 *Proc. Natl. Acad. Sci. USA* **84** 7024
[24] Ma J, Bai L and Wang M D 2013 *Science* **340** 1580
[25] Ma J, Tan C, Gao X, Fulbright R M Jr, Roberts J W and Wang M D 2019 *Proc. Natl. Acad. Sci. USA* **116** 2583
[26] Ma J and Wang M D 2016 *Biophys. Rev.* **8** 75